Environment International 166 (2022) 107348

Contents lists available at ScienceDirect

Environment International

journal homepage: www.elsevier.com/locate/envint

Full length article

Beyond green environments: Multi-scale difference in human exposure to greenspace in China

Bin Chen [a,b,c,*], Ying Tu [d], Shengbiao Wu [a], Yimeng Song [e,f], Yufang Jin [g], Chris Webster [c,h], Bing Xu [d], Peng Gong [b,i]

[a] Future Urbanity & Sustainable Environment (FUSE) Lab, Division of Landscape Architecture, Faculty of Architecture, The University of Hong Kong, Hong Kong Special Administrative Region
[b] Institute for Climate and Carbon Neutrality, The University of Hong Kong, Hong Kong Special Administrative Region
[c] Institute of Data Science, The University of Hong Kong, Hong Kong Special Administrative Region
[d] Department of Earth System Science, Ministry of Education Key Laboratory for Earth System Modeling, Institute for Global Change Studies, Tsinghua University, Beijing, China
[e] Department of Land Surveying and Geo-Informatics, The Hong Kong Polytechnic University, Hong Kong Special Administrative Region
[f] School of the Environment, Yale University, New Haven, CT, USA
[g] Department of Land, Air and Water Resources, University of California, Davis, CA, USA
[h] HKUrbanLabs, Faculty of Architecture, The University of Hong Kong, Hong Kong Special Administrative Region
[i] Department of Geography, and Department of Earth Science, The University of Hong Kong, Hong Kong Special Administrative Region

ARTICLE INFO

Handling Editor: Adrian Covaci

Keywords:
Green spaces
Environmental exposure
Population-weighted exposure
Urbanization
Environmental justice

ABSTRACT

Greenspace exposure metrics can allow for comparisons of green space supply across time, space, and population groups, and for inferring patterns of variation in opportunities for people to enjoy the health and recreational benefits of nearby green environments. A better understanding of greenspace exposure differences across various spatial scales is a critical requirement for lessening environmental health disparities. However, existing studies are typically limited to a single city or across selected cities, which severely limits the use of results in measuring systemic national and regional scale differences that might need policy at above individual city planning level. To close this knowledge gap, our study aims to provide a holistic assessment of multi-scale greenspace exposure across provinces, cities, counties, towns, and land parcels for the whole of China. We mapped the nationwide fractional greenspace coverage at 10 m with Sentinel-2 satellite imagery, and then modeled population-weighted greenspace exposure to examine variation of greenspace exposure across scales. Our results show a prominent scaling effect of greenspace exposure across multi-scale administrative divisions in China, suggesting, as expected, an increase in heterogeneity with finer spatial scales. We also identify an asymmetric pattern of the difference between greenspace exposure and greenspace coverage, across a geo-demographic demarcation boundary (i.e., along the Heihe–Tengchong Line). In general, the greenspace coverage rate will overestimate more realistic human exposure to greenspace in East China while underestimating in West China. We further found that, in China, more recently urbanized areas have much better greenspace exposure than older urban areas. Our study provides a spatially explicit greenspace exposure metric for discovering multi-scale greenspace exposure difference, which will enhance governments' capacity to quantify environmental justice, detect vulnerable greenspace exposure risk hotspots, prioritize greenspace management at the supra-city scale, and monitor the balance between greenspace supply and demand.

1. Introduction

Green spaces, typically open and undeveloped lands with natural vegetation such as parks, gardens, street plantation, lawns, forests, and crops (Mitchell and Popham, 2008; Wolch et al., 2014), provide critical ecosystem services to the function of the living environment (Wolch et al., 2014; Young, 2010). At a broad scale, greenspaces such as forests play an important role in the climate system by regulating the land–atmosphere exchange of energy and water (Friedlingstein et al., 2020; Zhao and Jackson, 2014). At local and urban scales, extensive studies

* Corresponding author.
E-mail address: binley.chen@hku.hk (B. Chen).

https://doi.org/10.1016/j.envint.2022.107348
Received 13 January 2022; Received in revised form 2 June 2022; Accepted 10 June 2022
Available online 14 June 2022

have documented a wide range of environmental benefits such as adjusting microclimate (Maimaitiyiming et al., 2014; Sun et al., 2019), reducing heat island intensity (Doick et al., 2014), mitigating air pollutions (Kumar et al., 2019; Nowak et al., 2014), and conserving biodiversity (Melero et al., 2020; Strohbach et al., 2013). Furthermore, the protective effects of urban greenspace on human health and mental wellness have been also widely reported (Sarkar et al., 2018), stemming from its functional roles in facilitating physical activity, supportive social interaction, promoting a sense of community, and stress-relief (Francis et al., 2012; Jiang et al., 2016; Kemperman and Timmermans, 2014; Kumar et al., 2019; Markevych et al., 2017; Sarkar et al., 2018).

Many parts of the world have gone through rapid population growth and urban expansion in the past half-century (Gong et al., 2020b; Gong et al., 2012), and this unprecedented urbanization process, driven by massive rural-to-urban migration, has led to substantial land cover modifications including destruction and modification of green spaces (Chen et al., 2017; Theobald et al., 2020). For instance, Nowak and Greenfield (2012) found 17 out of the 20 analyzed cities in the United States experienced significant declines in tree cover, with a decrease rate of 0.27% per year on average. A similar trend of consistent decline in urban greenspaces has been identified in most East European cities (Kabisch and Haase, 2013). In China, both Sun et al. (2011) and Chen et al. (2017) report a reduction in urban greenspace coverage in the major cities. Zhao et al. (2013) and Yang et al. (2014), however, conclude that Chinese cities have become greener since the 1990s. The main reason for this discrepancy seems to be differences in definitions of urban greenspaces (Chen et al., 2017). Urban greenspace can be either narrowly regarded as outdoor places with significant amounts of vegetation (Jim and Chen, 2003) or broadly represent any land that is partly or completely covered with grass, trees, shrubs, and other vegetation (Cameron and Hitchmough, 2016; Chen et al., 2017). Compounding the measurement problem, the inconsistent definition of urban extent and differences in spatial resolution of data sources lead to estimation bias and comparability and reliability problems. In addition to the observed trend of greenspace loss within cities, the rapid urbanization also modifies regional greenspace landscapes by converting agricultural land to urban uses (Tu et al., 2021). Given what we now know about the associations between green space, human health and wellbeing, the dramatic changes of green spaces accompanying the spread and intensification of cities is of great concern (Ezzati et al., 2018).

Greenspace privilege in terms of environmental justice is an increasing concern among academia, practice, and the public (Jennings et al., 2012; Rutt and Gulsrud, 2016; Wolch et al., 2014). In countries such as the United States (Lu et al., 2021; Rigolon et al., 2018), Germany (Wüstemann et al., 2017; Xu et al., 2018), and China (Song et al., 2021; Wu and Kim, 2021), strong disparities in greenspace supply have been observed across cities and communities. Gini coefficients are widely used to measure the inequality in greenspace accessibility within and across cities. Wu and Kim (2021) developed an urban greenspace equality index using Gini coefficients (UGSE) to measure the overall distribution of green spaces within a city and used a park green space equality index (PGSE) to measure equality of public access to parks. Results from 341 prefecture-level cities of China revealed strong disparities in both UGSE and PGSE. By further accounting for human mobility in greenspace exposure assessment across 303 cities in China, Song et al. (2021) reported that the majority of Chinese cities experienced a high inequality in urban greenspace exposure, with 207 cities having a Gini index larger than 0.6. Such findings should be informing governments and practitioners in optimizing greenspace management in pursuit of environmental justice and urban efficiency.

Despite a growing number of studies focusing on mapping, monitoring, and modelling of greenspace exposure, research advances are still limited. First, the spatial interaction between green spaces and humans has not been well quantified. The widely used indicators of greenspace coverage in total does not factor in accessibility to the population that might use it. Aggregate-level measures of total supply or per capita supply make an ecological fallacy. Per capita levels cannot account for spatial heterogeneity in greenspace demand from residents living in different places. Interaction indicators of exposure of this nature can be made more accurate by using network distance rather than crow-flies distance; weighting by demographic structure; and more nuanced calibrations made using social media data. Although some previous efforts have attempted to address these issues by considering the spatiotemporal dynamic of humans and the living environment (Chen et al., 2018a; Chen et al., 2018b; Song et al., 2018), they are limited to sampled cities because of obstacles in data availability and model generalization.

Second, the multi-scale difference of greenspace exposure has not been well disentangled. A better understanding of greenspace exposure differences across various spatial scales is a critical requirement for lessening environmental health disparities (Addas and Maghrabi, 2022; Collins et al., 2020; Labib et al., 2020) and optimizing urban planning practices (Chi et al., 2020; Liu et al., 2020; Sathyakumar et al., 2019; Wang et al., 2020). Existing studies of greenspace exposure assessment are typically constrained to a single city or sample of cities (Chen et al., 2020; Song et al., 2021; Song et al., 2018), rather than upscaling to a broader scale (e.g., province and country) or downscaling to finer scales of county, town, and land parcel. In addition, the scaling effect of buffer distances in incorporating different nearby green spaces for greenspace exposure assessment has not been disseminated from local to regional scales. However, multi-scale information regarding the spatial heterogeneity of human exposure to greenspace is very important to governments at all levels from central to local policymakers, for practical improvements in greenspace planning.

Third, existing knowledge about greenspace exposure is intensively clustered in the urban context, with limited studies quantifying the spatial gradient in greenspace exposure among different stages or levels of urbanization (e.g., different size or tiers of city). A quantitative analysis addressing this issue will advance our understanding of greenspace environments and greenspace exposure differences regarding cross-sectional contexts, and better inform policies and actions in a policy setting like China, where urbanization is continuously an active dimension of policy and planning (Mu et al., 2020; Zhou et al., 2021). Our study is thus designed to move from policy evaluation and needs assessment of specific cities, to attempt to lay a foundation for a science of greenspace exposure across the entire urban density spectrum.

To our best knowledge, no other empirical study has yet examined the multi-scale differences of human exposure to greenspace in a nationwide context across a country's complete urban density gradient. In addition, previous efforts led by local agencies and governments for greenspace mapping and greenspace exposure assessment have often yielded different results with unexplainable differences because of inconsistent measurement and modelling methods. It is critical to make greenspace exposure assessments at multiple scales that are derived from the same or consistent data sources with the same or compatible mapping and assessment methods. This is because, only with greenspace exposure assessment results and baselines derived from similar criteria, can consistent environmental policies be made, and adaptative action efforts be compared and assessed for multi-level stakeholders and environmental administrations (Gong et al., 2020a).

In view of the abovementioned challenges, our study develops a multi-dimensional framework to characterize the spatial interaction between humans and green spaces; quantifies multi-scale exposures; and as a proof-of-concept experiment, uses it to classify the underlying patterns and characteristics in greenspace exposure across the whole of China. Specifically, we address the following three questions: (1) What are the differences in human exposure to green spaces across province-, city-, county-, town-, and parcel-level assessments? (2) How do the distributions of greenspace coverage and greenspace exposure compare throughout China? and (3) How does urban expansion impact the distribution of greenspace exposure over space and time?

2. Methods

2.1. Study design

Fig. 1 presents the flowchart of research data, methods and expected results in this study. We measured interaction between greenspace coverage and population distribution as an indicator of both human exposure to greenspace in China and demand–supply relationship. Specifically, we used Sentinel-2 imagery and spectral unmixing to generate fractional greenspace coverage and leveraged PlanetScope high-spatial-resolution imagery for accuracy validation. We used WorldPop for an estimate of the spatial distribution of population, and the corresponding census data for accuracy validation. Based on the population-weighted exposure models, we conducted a multi-scale greenspace exposure assessment across unit divisions of province, city, county, town, and land parcel. We visualized results using the WebGIS platform. Based on these data, we investigated multi-scale difference of greenspace exposure across China, with explicit controls of space and scale in data attributes.

2.2. Generation of greenspace fraction map in China

We adopted a linear spectral unmixing (LSU) model to map a 10-m fractional greenspace coverage map in China for the baseline year—2020, on the Google Earth Engine (GEE) platform, using a total of 240,190 Sentinel-2A/B images during the temporal period (January 2019 to December 2020). The LSU model is a subpixel analytical method that decomposes a mixed pixel into a group of fractions using pure land-cover pixels-'endmembers' (Keshava, 2003). Different from conventional pixel-based methods, subpixel methods can tackle the mixed pixel problem of moderate and coarse resolution remote sensing data and have shown great potential in greenspace mapping (Song et al., 2021; Song et al., 2020). As expressed in Eq. (1), the LSU model assumes that the spectral signature of each pixel can be modeled as a linear combination of a few spectrally pure land-cover components (Weng et al., 2004).

$$R_{ib} = \sum_{k=1}^{n} f_{ki} \cdot C_{kb} + \varepsilon_{ib} \quad (1)$$

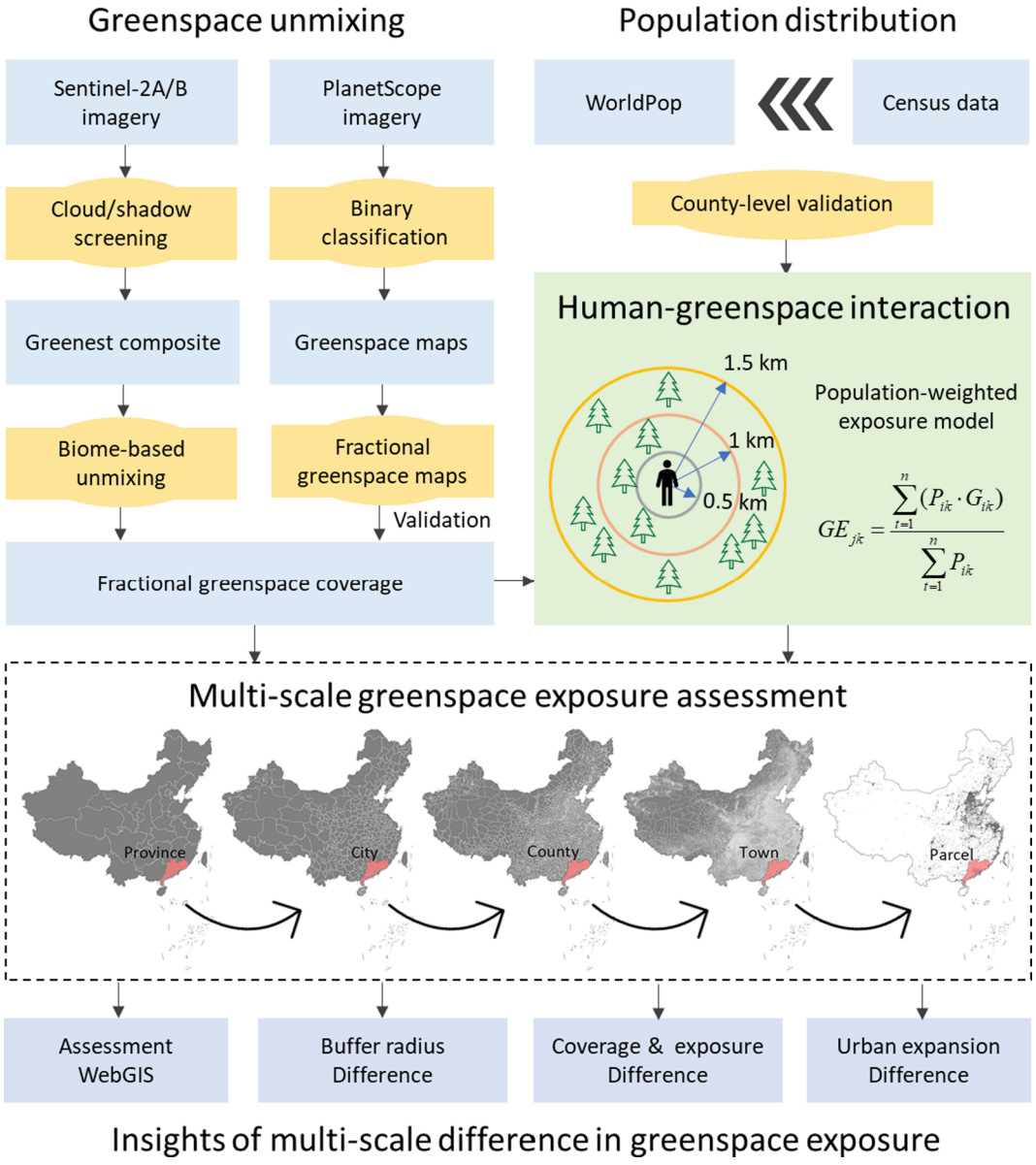

Fig. 1. Flowchart of study design, including dataset, methods, and expected results.

where R_{ib} denotes the spectral reflectance for band b in the ith pixel covered by one or more pure land-cover endmembers, f_{ki} is the proportion of endmember k in the ith pixel, C_{kb} is the known reflectance of endmember k in band b, ε_{ib} is the unmodeled residual in the ith pixel, and n represents the total number of endmembers. The proportion f_{ki} is subject to the following constraints in Eqs. (2)–(3), which can be calculated using the least-squares method.

$$\sum_{k=1}^{n} f_{ki} = 1 \tag{2}$$

$$0 \leqslant f_{ki} \leqslant 1 \tag{3}$$

Given the limitation of the maximum computation capacity of GEE, we divided the entire study area into $3^\circ \times 3^\circ$ subregions (140 subregions in total) for extracting greenspace fraction maps (Fig. S1B). Within each subregion, we built an LSU model based on the biome's endmember library, and then unmixed the composited Sentinel-2 image to estimate fractional greenspace coverage. We incorporated the four 10-m bands of Blue, Green, Red, and Near Infrared (NIR), and two additional bands of NDVI and NDWI as the input to the LSU models. Finally, we used the high-resolution PlanetScope imagery as reference to validate the derived fractional greenspace coverage maps. Methodological details of data pre-processing, endmember section, greenspace unmixing, and validation are provided in Supplementary Materials.

2.3. Gridded population dataset

WorldPop (www.worldpop.org) provides the estimated number of people residing in each 100 m × 100 m grid based on a Random Forest model and a global database of administrative unit-based census (Stevens et al., 2015). Given the superiority of its fine spatial resolution and yearly updated frequency over other grid-based population datasets such as the Gridded Population of the World (GPW) (CIESIN, 2018) and LandScan (Dobson et al., 2000), we used the WorldPop dataset in 2020 to quantify the spatially-explicit distribution of population in China. We further collected the population census of China in 2014 obtained from the national scientific sharing platform for population and health (www.ncmi.cn) to validate the accuracy of WorldPop dataset at the county-level scale. We measured a relatively plausible validation performance with R-square above 0.9 (Fig. S2).

2.4. Hierarchy of unit division

Since greenspace and population distribution vary across space, the spatial heterogeneity of both should be assessed when estimating greenspace exposures. This should be done at different spatial scales because of the modifiable areal unit problem (MAUP) (Chen et al., 2018b). Measuring at multiple spatial scales is a measurement reliability test that may yield insights into scale-specific patterns and dynamics in relation to exposure.

We therefore used four different administrative division boundaries as the spatial unit of analysis for greenspace exposure: province-level administrative division boundaries (hereafter "province", Fig. 1), prefecture-level city administrative division boundaries (hereafter "city", Fig. 1), county-level city administrative division boundaries (hereafter "county", Fig. 1), and town-level administrative division boundaries (hereafter "town", Fig. 1).

In addition, land parcels that represent homogeneous socioeconomic functions (Gong et al., 2020a), were adopted to evaluate greenspace exposure at a finer scale. We used major roads and minor roads from OpenStreetMap (OSM) data (www.openstreetmap.org) as the road network to divide land parcels across the whole of China. Spatially, land parcels are polygons bounded by road networks, which serve as the intrinsic segmentation of urban land use functions (Gong et al., 2020a). We further removed those small parcels with a total area of less than 1000 m^2. By overlaying the parcel map with a global urban boundary (GUB) extracted from Landsat data in 2018 (Li et al., 2020), we generated a final land parcel layer for the finest level of greenspace exposure assessment (Fig. 1).

2.5. Greenspace coverage assessment

We calculated the physical greenspace coverage (GC) rate by overlapping greenspace fraction maps derived from Section 2.2 with different unit division schema in Section 2.4. The mean GC for each unit across different scales can be derived according to Eq. (4),

$$GC = \frac{\sum_{i=1}^{N} G_i}{N} \tag{4}$$

where G_i represents the greenspace coverage fraction of ith grid, N is the total of grids within the specific unit, and GC is the estimated greenspace coverage level for the corresponding unit.

2.6. Population-weighted greenspace exposure assessment

We calculated population-weighted greenspace exposure of varying buffer sizes for each unit division (from Section 2.4). The population-weighted exposure model is a bottom-up assessment (Chen et al., 2018a; Chen et al., 2018b; Song et al., 2018), which considers the spatial interaction between population distribution and greenspace allocation by giving proportionately greater weight to greenspace exposure where more people live. Specifically, the population-weighted exposure to greenspace of different buffer sizes in each unit division GE^b is defined as below.

$$GE^b = \frac{\sum_{i=1}^{N} P_i \times G_i^b}{\sum_{i=1}^{N} P_i} \tag{5}$$

where P_i represents the population of ith grid, G_i^b represents the fractional greenspace cover of the ith grid at the varying buffer size of b (i.e., 100 m, 500 m, 1000 m, and 1500 m in this study). N denotes total number of grids within the specific unit.

2.7. Multi-scale difference in greenspace exposure

Based on the GE index described in Section 2.6, we first built an ESRI-empowered WebGIS-based platform to visualize the difference in GE across different division schemas. We investigated the difference in greenspace exposure across scale and space with the following research emphasis.

2.7.1. How does the buffer radius of nearby green environments impact greenspace exposure assessment?

Varying buffer radius provides a dynamic view of the spatial heterogeneity of human-greenspace arrangement. We used four buffer radiuses of 100, 500, 1000, and 1500 m to calculate population-weighted greenspace exposure and investigated how the buffer radius of nearby green environments would impact greenspace exposure assessment. Specifically, we calculated the difference between scenarios with 1500-m and 500-m buffer radiuses to measure the bounding range of greenspace exposure experience across different division schemas. Additionally, previous studies have widely used a quarter mile (400–500 m) neighborhood for measuring greenspace exposure (Sarkar et al., 2018). We therefore selected a 500-m catchment buffer for our main analysis (results based on the other three buffer radiuses are provided in Supplementary Materials).

2.7.2. How do the distributions of greenspace coverage and greenspace exposure compare throughout China?

By definition, greenspace coverage amount and distribution is not

equal to greenspace exposure (Song et al., 2021; Song et al., 2018) since the latter seeks to index demand while the latter indexes supply only. Technically speaking, the difference between greenspace coverage and greenspace exposure for a single cell is cell population. But aggregated to an administrative unit of analysis, the difference is not deterministic and will be co-controlled by the spatial distribution of greenspace and population. For example, if the physical greenspace coverage (GC) of one city is 60%, it means that the total greenspace coverage divided by the total city area is 60%. In contrast, if the greenspace exposure (GE) is 60% (let's say using the nearby 500-m buffer zone in Eq. (5)), it means that the greenspace coverage within people's nearby 500-m environment is 60% on average for this city. We therefore ask how does this difference vary across spatial locations? By calculating the physical GC in Section 2.5 and comparing it with the corresponding population-weighted GE in Section 2.6, we quantified the difference between GC and GE for four administrative division schemas. We further summarized these differences over seven regional zones of North China (NC), Northeast China (NEC), East China (EC), Central China (CC), Southwest China (SC), Northwest China (NC), South China (SC) (Fig. S1B).

2.7.3. How does urban expansion impact greenspace exposure over space and time?

Urban expansion has greatly reshaped the national greenspace landscape of China, but how urban expansion impacts the distribution of greenspace exposure over space and time remains unclear. We collected GUB data in 1990, 2000, 2010, and 2018 to divide the entire urban area of China into urban expansion periods (Li et al., 2020). We first categorized it into two: old urban areas (before 1990), and new urban areas (from 1990 to 2018); and then further categorized new urban areas into three groups: early-stage new urban (from 1990 to 2000), middle-stage new urban (from 2000 to 2010), and recent new urban (from 2010 to 2018). We employed the population-weighted greenspace exposure model in Eq. (5) to calculate mean greenspace exposure level for each category. We also overlapped the GUB-based urban expansion profiles with province divisions to investigate the impact of urban expansion on greenspace exposure at the province level.

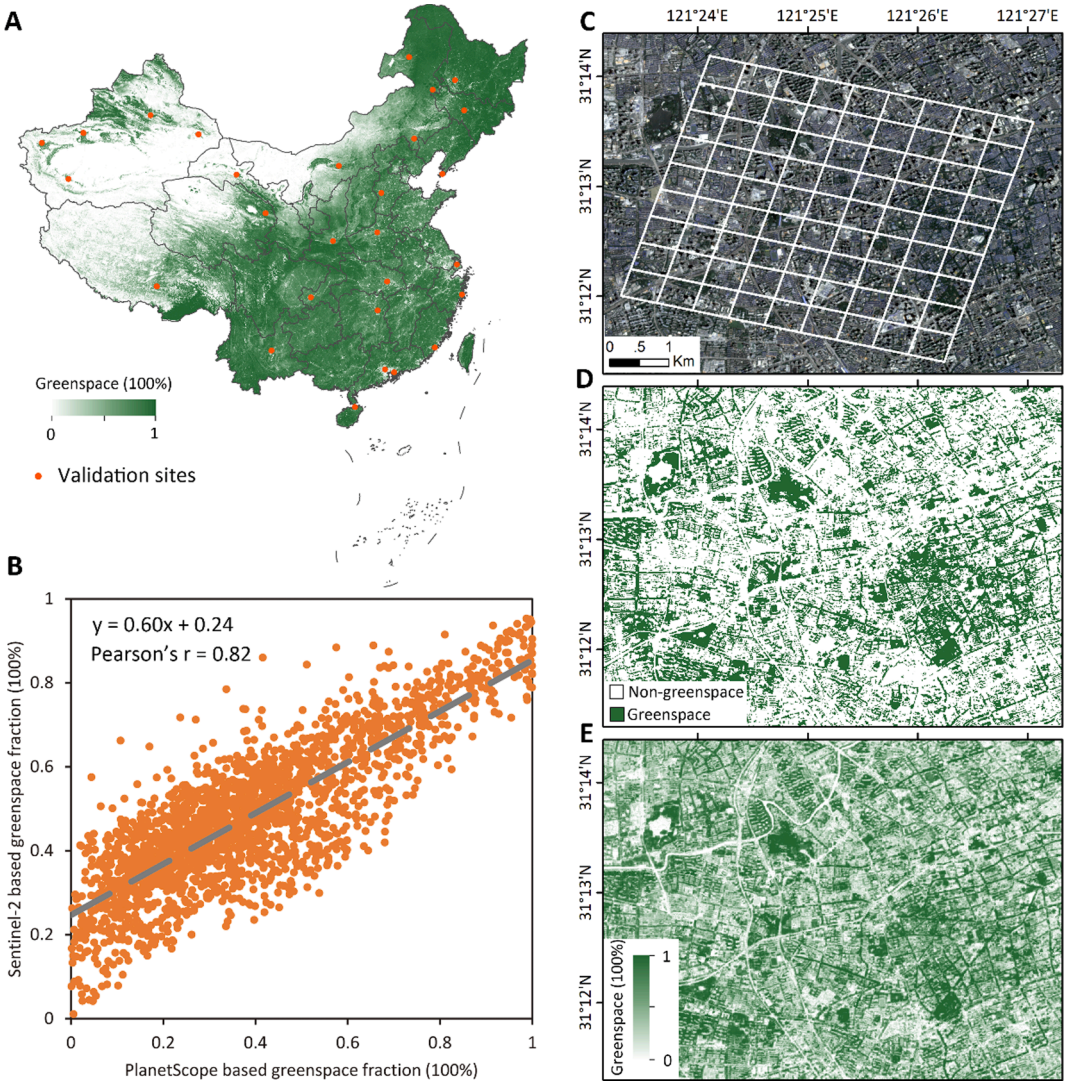

Fig. 2. Mapping and validation of greenspace fractional maps. (A) Geographic distribution of the maximum greenspace fractional coverage, overlaid with 27 validation sites in China, (B) comparison between PlanetScope based greenspace fraction versus Sentinel-2 based greenspace fraction, (C) the Red-Green-Blue composite of PlanetScope imagery, (D) PlanetScope based greenspace/non-greenspace classification, and (E) Sentinel-2 based greenspace unmixing results in Shanghai.

3. Results

3.1. Mapping and validation of fractional greenspace coverage

Fig. 2A presents an unmixing-based fractional greenspace coverage map (which was aggregated to 1000 m for visualization). With validation sites distributed across China (Fig. 2A), the derived greenspace coverage maps achieve a relatively high correlation coefficient of 0.82, with respect to greenspace coverage derived from the high-spatial-resolution PlanetScope imagery (Fig. 2B). Regarding the spatial distribution of greenspace coverage, the Sentinel-2 unmixing-based fractional greenspace coverage (Fig. 2E) shows a very consistent pattern with the classification-based greenspace coverage derived from PlanetScope imagery (Fig. 2C-D).

3.2. Spatial heterogeneity of greenspace exposure assessment

Fig. 3 shows the assessment of human exposure to greenspace in China at multiple scales of province (Fig. 3A), city (Fig. 3B), county (Fig. 3C), and town (Fig. 3D). On the one hand, for each scale, there is a prominent geographical difference in the magnitude of greenspace exposure. For example, as for province-level assessment, Guizhou (70.28%), Heilongjiang (69.20%), Yunan (68.63%), and Guangxi (67.78%) are the leading provinces with relative high greenspace exposure levels. In contrast, provinces distributed in coastal regions of southeast China and arid/semi-arid regions of northwest China are characterized with lower greenspace exposure levels. On the other hand, among different scales, there are also obvious differences in geographical pattern and magnitude of greenspace exposure. By diving into a finer-scale greenspace exposure assessment results, we identify more spatial heterogeneity of greenspace exposure, for example, within a province (Fig. 3A-B), a city (Fig. 3B-C), and a county (Fig. 3C-D).

Fig. 4 presents an extracted example in Beijing to illustrate how the derived assessment results can be used to provide thematic information that documents different facets of human exposure to greenspace. As an entire unit of a city, Beijing is featured with an overall greenspace exposure level of 46.72% (Fig. 4A). In other words, the greenspace coverage within people's nearby 500-m environment is 46.72% on average in Beijing. With the scope of Beijing's 16 counties (Fig. 4B), suburban counties such as Yanqing (60.77%), Fangshan (58.77%), Miyun (56.70%), and Huairou (55.50%) are the leading ones with highest greenspace exposure levels, while core counties such as Xicheng (34.15%) and Dongcheng (35.91%) have lower greenspace exposure. At the town-scale (Fig. 4C), more detailed heterogeneities in greenspace exposure levels can be differentiated. In particular, parcel-level greenspace exposure reveals detailed greenspace exposure difference at an urban design scale, corresponding roughly to neighborhood communities. Fig. 4D identifies which neighborhood land parcels enjoy better greenspace exposure relative to others in Beijing.

As expected, and by deduction, our results reveal that a larger buffer

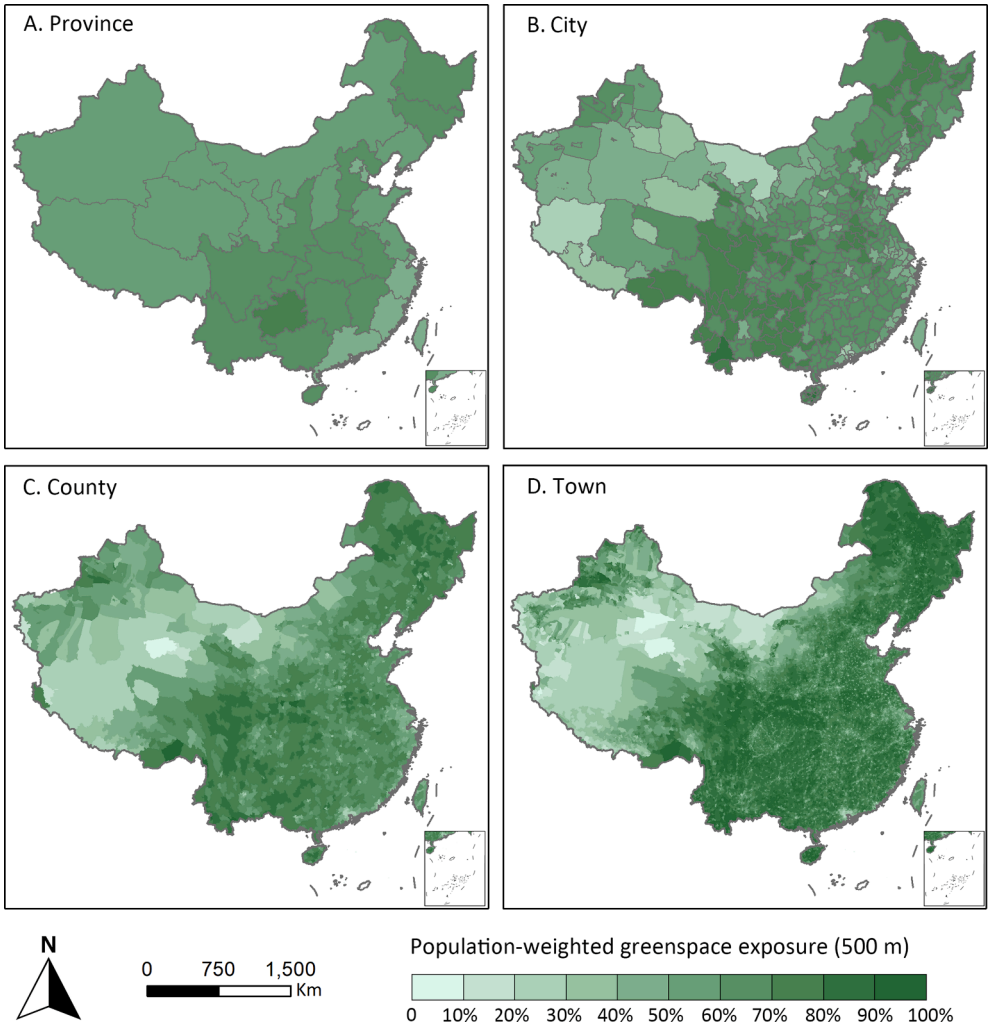

Fig. 3. Multi-scale assessment of human exposure to greenspace in China, using 500-m radius as the buffered neighborhood environment. Statistics of greenspace exposure levels at different administrative divisions of (A) province, (B) city, (C) county, and (D) town.

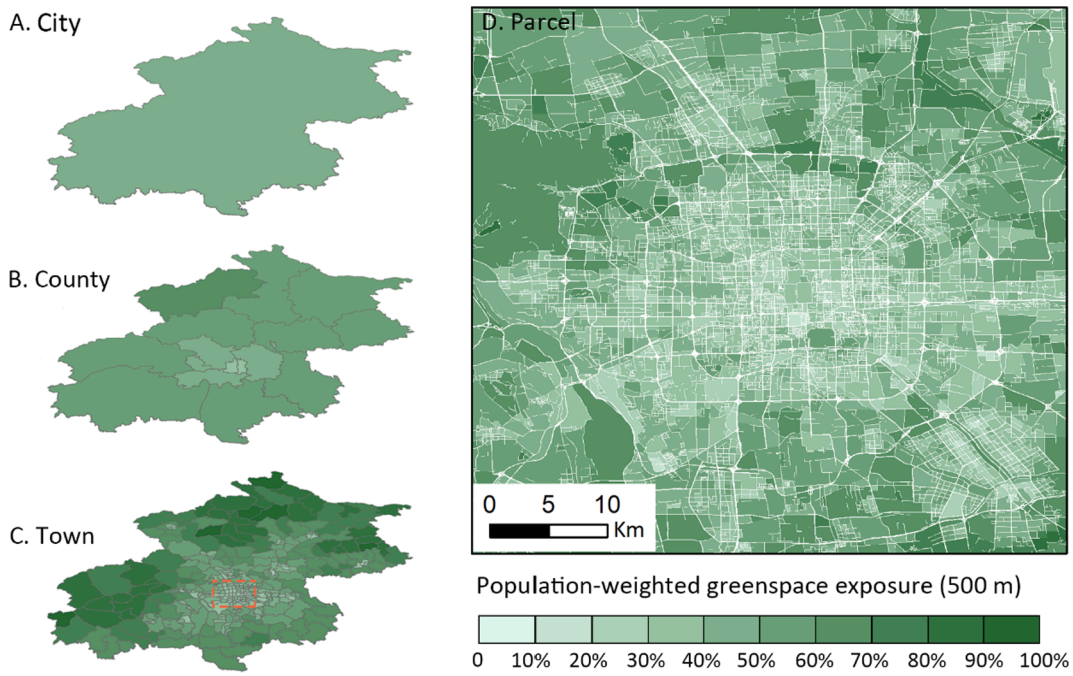

Fig. 4. Multi-scale assessment of human exposure to greenspace, using Beijing as an example. Statistics of greenspace exposure levels at different scales of (A) city, (B) county, (C) town, and (D) parcel.

radius will lead to an increased greenspace exposure assessment, because more remote greenspace coverages can be taken into consideration for the exposure assessments. Another observation is that broader-scale assessments conducted at the scales of province, city, and town are more robust to the changing buffer radiuses, with an averaged difference of 1.8%, 1.9%, and 2.0%, respectively (Fig. 5). However, when we investigate the finer-scale assessments using towns and parcels, the derived assessments yield more heterogeneities, as witnessed from the larger standard deviations (Fig. 5).

In the example of Beijing (Fig. 6), we observe contrasting greenspace exposure levels among different land parcels, using a 100-m buffer radius for Eq. (5) (Fig. 6A). For instance, there are several parcels colored dark red, with averaged greenspace exposure levels less than 10%. In contrast, there are some land parcels colored blue with averaged greenspace exposure levels higher than 60% or 70%. This disparity will, however, be significantly mitigated by incorporating more nearby green spaces when using the 500-m buffer radius for greenspace exposure assessments (Fig. 6B). By further lifting the buffer radius to 1000 m and 1500 m, we will find that the majority of land parcels are within the category of greenspace exposure levels from 30% to 40% (Fig. 6C-D). However, we find some clusters of land parcels with a consistent lower greenspace exposure across buffer radiuses (e.g., colored in orange with averaged greenspace exposure levels from 20% to 30%). This finding can help identify vulnerable localities or regions facing limited nearby greenspaces in relation to population size. More importantly, the clustering of greenspace exposure serves as a spatially explicit reference to inform policymakers and planners to prioritize greenspace supply and optimize greenspace settings, targeting the most fundamental issue of balancing greenspace supply and demand.

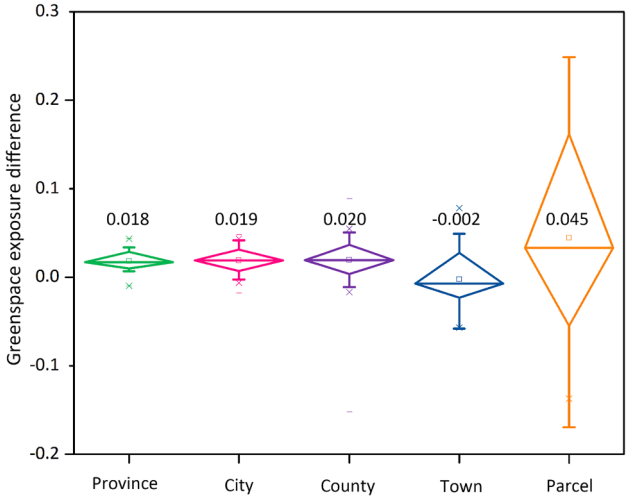

Fig. 5. Boxplot of greenspace exposure differences between assessment results using 1.5-km and 0.5-km buffer radius across five division scales from province to city, county, town, and parcel. The labeled numbers are the mean values for greenspace exposure difference for each statistical level.

3.3. Difference between greenspace exposure and greenspace coverage

To compare population-weighted greenspace exposure (Fig. 3) and greenspace coverage rate (Fig. S6), we generated differences across China at the following scales: province, city, county, and town. The red color in Fig. 7 represents locations where human greenspace exposure is lower than the physical greenspace coverage rate, and the blue color shows where human greenspace exposure is higher than the physical greenspace coverage rate. Results show that the commonly used indicator such as greenspace coverage rate, will both over- and under- estimate greenspace exposure at all scales of divisions. But the estimation error is not random. We identify an asymmetric pattern of differences between greenspace exposure and greenspace coverage, across a demographic demarcation boundary, i.e., at the two sides of Hu Line: Heihe–Tengchong Line in China (Hu, 1935). Specifically, East China is characterized by 'overestimation' such that human greenspace exposure is lower than physical greenspace coverage rate, while West China is characterized by 'underestimation', where human greenspace exposure is higher than physical greenspace coverage rate. This pattern is particularly prominent at the scales of province (Fig. 7A) and city (Fig. 7B). Nevertheless, we can also observe some 'overestimation' regions in West China and some 'underestimation' regions in East China if

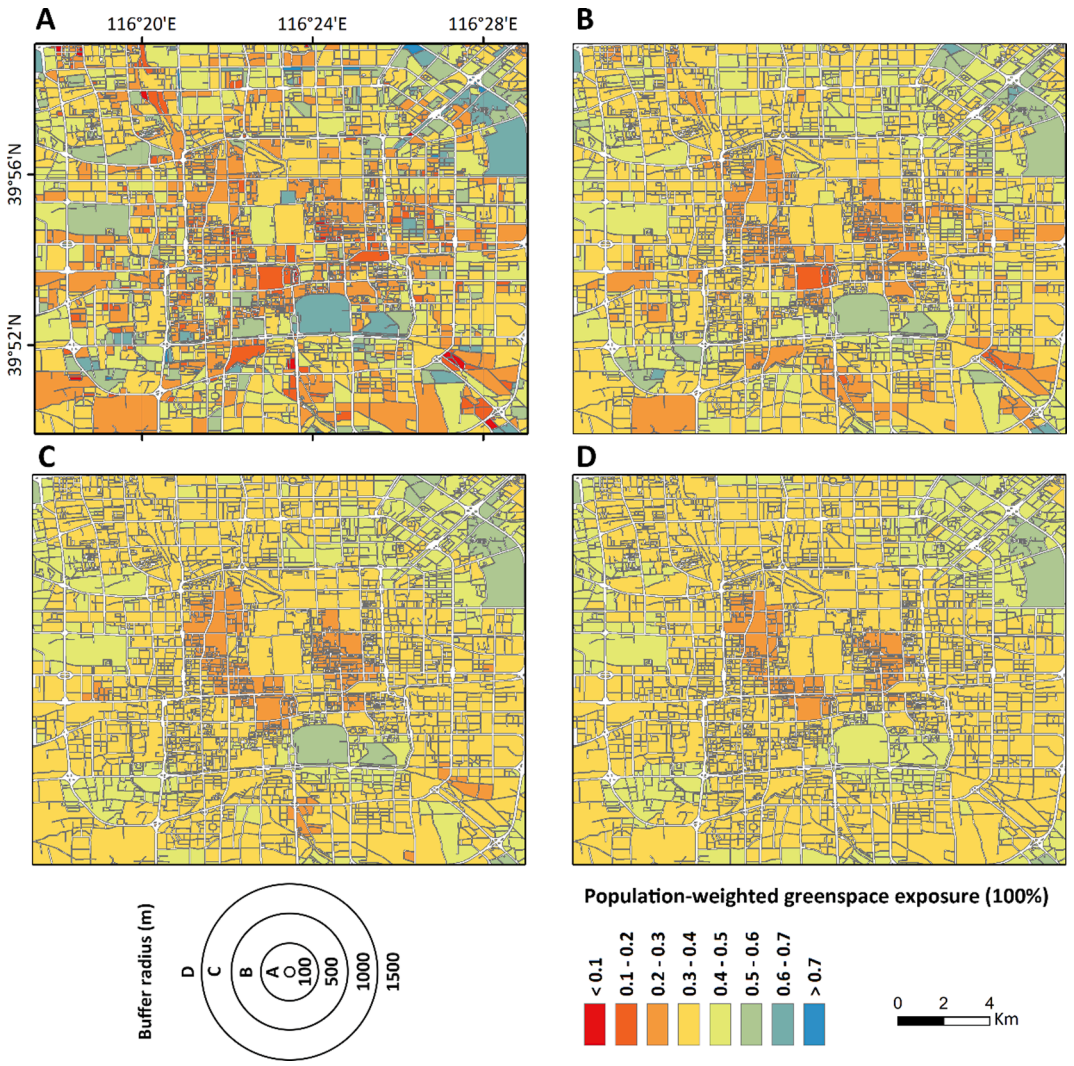

Fig. 6. Comparison of population-weighted greenspace exposure assessment results using different buffer radiuses. Examples of parcel-level assessments in Beijing using (A) 100 m, (B) 500 m, (C) 1000 m, and (D) 1500 m.

we investigate at finer scales of county (Fig. 7C) and town (Fig. 7D).

Statistics at individual regional zones further suggest a considerable difference between greenspace exposure and greenspace coverage in China (Table 1). Except for Northwest China (0.41 ± 14.59%), the remaining six regional zones all have greenspace exposure below greenspace coverage at the city scale, with mean differences of −12.00 ± 10.88% for North China, −21.20 ± 6.67% for Northeast China, −15.93 ± 6.97% for East China, −13.46 ± 4.02% for Central China, −10.29 ± 8.61% for Southwest China, and −16.78 ± 6.81% for South China. As for the county scale, all regional zones show a negative difference on average between greenspace exposure and greenspace coverage (Table 1). As for the town scale, the pattern of difference was the same as that at city scale (Table 1).

3.4. Impact of urban expansion on greenspace exposure

China has witnessed unprecedented urban expansion over the past three decades (Gong et al., 2020b). As shown in Fig. 8A, the extracted example in Beijing outlines the progress of urban expansion over different temporal periods, i.e., blue colors represent the old urban areas before 1990, orange colors represent early-stage expanded urban areas between 1990 and 2000, green colors represent middle-stage expanded urban areas between 2000 and 2010, and pink colors represent recent expanded urban areas between 2010 and 2018. It is clear to see that compared to the period 1990–2000, the subsequent two decades (2000–2010 and 2010–2018) experienced much more extensive urban expansion (Fig. 8A). By treating urban areas before 1990 as old urban areas and grouping the expanded urban areas from 1990 to 2018 as the new urban areas, our results show that as a whole in China, residents living in the new urban areas enjoy better greenspace exposure (41.47%), which is 9.08% higher than residents living in the old urban areas (32.39%). By dividing the urban expansion into four temporal periods, we find a clear trend of increased greenspace exposure from old to newest urban areas (Fig. 8B), i.e., from old urban areas (32.39%) to early-stage expanded urban areas (34.68%), middle-stage expanded urban areas (41.20%), and recent expanded urban areas (51.98%). Results at the province scale further reinforce the finding that compared to the old urban areas, recent newly expanded urban areas are providing better greenspace exposure for residents (Fig. 8C).

4. Discussion

4.1. Scaling effect of greenspace exposure

Our study disentangles two aspects of multi-scale differences in human exposure to greenspace in China. (1) Greenspace exposure assessment with a top-down approach across different administrative units from province to city, county, town, and land parcel scales.

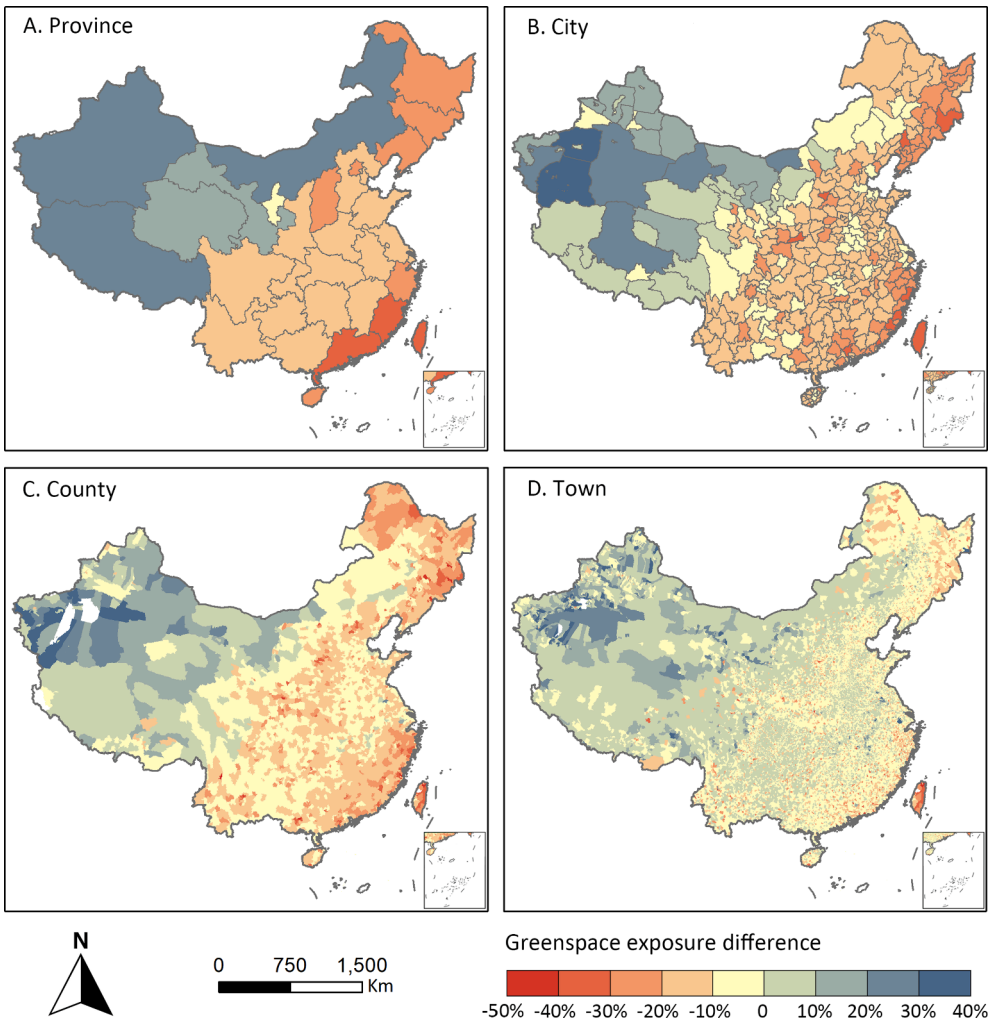

Fig. 7. Difference between population-weighted greenspace exposure and greenspace coverage rate (GE-GC) across different administrative divisions of (A) province, (B) city, (C) county, and (D) town.

Generally, the spatial heterogeneity of greenspace exposure is featured by three main characteristics. First, there is an asymmetric pattern of the differences between greenspace exposure and greenspace coverage (GE-GC) between the two sides of the Hu Line. East China has lower greenspace exposure than coverage, whereas West China has higher greenspace exposure than coverage (Fig. 7). This is because the arid and semi-arid environmental condition in West China makes it less suitable for vegetation growth. Available green is distributed much closer to human settlements (Song et al., 2020). This is presumably due both to human cultivation and irrigation around settlements and the attraction of humans to settle near cultivable land and water sources. Our indicator is therefore picking up the more efficient use of green space and irrigated or irrigable land in more arid regions, where it is scarcer. In contrast, there are plenty of forests distributed in remote areas far from human settlements in East China. Second, the spatial pattern of greenspace exposure has its distinctiveness for each scale. In particular, the spatial interaction between greenspace coverage and population distribution leads to the observed heterogeneity across different scales. For example, at the province scale, we will find Guizhou achieves the highest greenspace exposure level (Fig. 3A). But at city and county scales, we identify uneven distribution of greenspace exposure levels, with some cities and counties in Guizhou still experiencing lower greenspace exposure (Fig. 3C-D). There will be a greater heterogeneity because of the difference in human-greenspace distribution when we check at finer scales of town and parcel (Fig. 4). Third, there is a considerable difference in greenspace exposure within urban areas. Our results indicate that older urban areas are experiencing lower greenspace exposure than those newly expanded areas. This observation highlights the need for practicing actions to realize more equal greenspace exposure for urban residents by balancing the land supply and greenspace conservation. (2) Buffer size of nearby green environments in greenspace exposure assessment. Different buffer sizes that incorporate different ranges of nearby green environments will impact the outcomes of greenspace exposure assessment (Su et al., 2019), but this has not been quantitively assessed across spatial scales. The sensitivity analysis regarding buffer radiuses of people's nearby greenspace further helps reveal the local heterogeneity in human-greenspace relationship. The WebGIS-based platform built from this study provides a comprehensive view of multi-scale greenspace exposure with respect to multi-scale buffer radiuses as the neighborhood range of living neighborhood and physical accessibility.

4.2. *Contributions and implications*

As an empirical study, this work makes contributions to knowledge and practice that may be impactful to the field of green environments and shed potential light on future research, policymaking, planning, and design. First, we generated the factional greenspace coverage map at a spatial resolution of 10 m in China, which provides a very fine scale greenspace mapping that can account for subpixel greenspace

Table 1
Multi-scale statistics of greenspace coverage, greenspace exposure and the associated difference over seven zones in China. North China, Northeast China, East China, Central China, Southwest China, Northwest China, and South China.

Region	Greenspace coverage (%)	Greenspace exposure (%)	Difference (%)
(1) City level			
North China	69.29 ± 15.86	57.29 ± 10.20	−12.00 ± 10.88
Northeast China	86.95 ± 6.54	65.76 ± 7.43	−21.20 ± 6.67
East China	74.22 ± 8.91	58.29 ± 9.55	−15.93 ± 6.97
Central China	79.02 ± 6.02	65.56 ± 7.53	−13.46 ± 4.02
Southwest China	78.00 ± 13.96	67.71 ± 10.40	−10.29 ± 8.61
Northwest China	57.30 ± 22.16	57.71 ± 11.90	0.41 ± 14.59
South China	78.26 ± 14.06	61.48 ± 16.42	−16.78 ± 6.81
(2) County level			
North China	70.22 ± 13.81	59.84 ± 12.38	−10.38 ± 7.55
Northeast China	80.58 ± 15.88	64.68 ± 15.44	−15.90 ± 9.70
East China	70.68 ± 14.48	58.24 ± 13.23	−12.43 ± 7.86
Central China	74.80 ± 11.97	63.81 ± 13.01	−10.99 ± 5.69
Southwest China	75.83 ± 15.25	67.45 ± 13.94	−8.37 ± 8.11
Northwest China	60.81 ± 23.15	59.49 ± 14.94	−1.32 ± 13.96
South China	75.94 ± 15.39	61.24 ± 16.53	−14.70 ± 7.60
(3) Town level			
North China	67.57 ± 17.70	65.36 ± 17.56	−2.21 ± 5.53
Northeast China	74.37 ± 22.44	70.37 ± 21.48	−4.00 ± 6.97
East China	70.04 ± 18.00	66.54 ± 18.48	−3.50 ± 7.18
Central China	72.08 ± 17.62	70.05 ± 18.33	−2.03 ± 5.73
Southwest China	76.53 ± 14.96	75.54 ± 15.82	−0.99 ± 6.04
Northwest China	63.75 ± 21.36	64.52 ± 19.08	0.77 ± 8.65
South China	72.30 ± 20.50	67.80 ± 21.08	−4.50 ± 6.88

coverages. The classification-based methods and products have been widely used to extract greenspace coverages from moderate satellite imagery such as Landsat and Sentinel-2 (Chen et al., 2017; Kuang et al., 2021; Liou et al., 2021). However, this sort of hard classification will inevitably lead to biased estimations (over- or under-estimations) for those subpixel greenspace signals. The availability of commercial high-spatial-resolution imagery has contributed to the accurate extraction of greenspace coverage, but these efforts are always limited to local scales such as cities and urban agglomerations. As an optimal balance between mapping accuracy and financial costs, this study extended our previous efforts of Sentinel-2-based unmixing to derive national greenspace coverage mapping. The inclusion of an extensive group of validation plots from high-spatial-resolution PlanetScope imagery also verifies the robust and reliable performance of this derived dataset. Second, we considered the spatial structure of both greenspace coverage and population distribution to model the interaction between human and greenspace. This helps estimate the degree to which commonly used indicators such as greenspace coverage rate will overestimate or underestimate greenspace demand, measured by an exposure model. Although many previous studies have been working on greenspace assessment (Table S1), they are more in terms of greenspace supply measurement and limited by local to regional scales. The derived greenspace exposure metrics can allow for comparison of greenspace supply across space, and for inferencing variations in opportunities for people to enjoy the health and recreational benefits of nearby green environments. To our best knowledge, this study is the first effort to provide a multi-scale greenspace exposure assessment across four different administrative unit divisions and land parcels in China.

The data, methods, and results generated from this study are expected to have broader potential beneficiaries to practical implications. First, the direct deliverables including the national greenspace mapping and multi-scale greenspace assessment results provide evidence and insights for central and local governments, to have a better understanding of the physical greenspace arrangement and people's actual exposure to greenspace. This knowledge advanced by this study will help policymakers, urban planners, and landscape designers to implement more effective and sustainable greening programs adjusted to different local circumstances to achieve more equitable distributions of greenspace. For example, our results can provide spatially explicit guidance for relevant stakeholders to identify locations where supply should be improved for better greenspace exposure. Our model can be used even to calculate the magnitude of greening effort needed to reach certain thresholds or targets. Second, our multi-scale greenspace exposure assessment reveals that the physical greenspace coverage rate will overestimate the population-adjusted supply experience, especially for East China. It provides critical insights to incorporate more human-oriented indicators for measuring green cities. The spatial interaction between population distribution (i.e., location and density) and green environments (i.e., coverage and amount) should be considered to uncover how people are really enjoying nearby greenspace during their daily life.

4.3. *Uncertainties and future research*

Some uncertainties in this study should be acknowledged. First, the main analysis of this study uses the greenest composite to represent the maximum greenspace coverage. However, the difference in vegetation phenology throughout a year will impact people's cumulative greenspace exposure levels, especially for the latitudinal transect. Therefore, we incorporate the time-series Sentinel-2 imagery to derive the seasonal composites and further verify the seasonal changes of human exposure to greenspace (Supplementary Materials). Our analysis reveals that greenspace exposure is dynamic seasonally across province, city, county, and town (Fig. S7), with the largest magnitude between summer and autumn and much lower in spring and winter. Based on the difference in greenspace exposure between summer (i.e., the peak) and winter (i.e., the trough), as expected, we found a significant latitudinal gradient in China, where the northern China has much a larger seasonality in greenspace exposure than the southern part (Fig. S8). Nevertheless, the greenest composite in the main analysis provides an estimate of the maximum potential in greenspace exposure. Our next step is to incorporate long-term time-series remote sensing imagery to provide spatially and temporally explicit monitoring and mapping of greenspace, which can account for changes in both seasonal phenology and abrupt disturbances. Second, this study uses the satellite-based greenspace coverage to quantify human greenspace exposure, without differentiating greenspace type and quality. However, human exposure to different greenspace types such as tree (shadowed) and shrub/grass (non-shadowed) has been associated with different health benefits (Reid et al., 2017). Additionally, the top-down estimate of greenspace amounts cannot accurately depict eye-level greenspace appreciation, which will generate certain differences (Jiang et al., 2017). Addressing this issue, one of our suggestions for future research is to combine multi-source remote sensing and social sensing datasets, such as satellite, Lidar, StreetView imagery, and crowdsourcing panorama images to derive greenspace type classification and model the transformation functions between 'bird-view' and 'eye-view' greenspace. Lastly, this study used the buffer radius to quantify people's nearby greenspace environments.

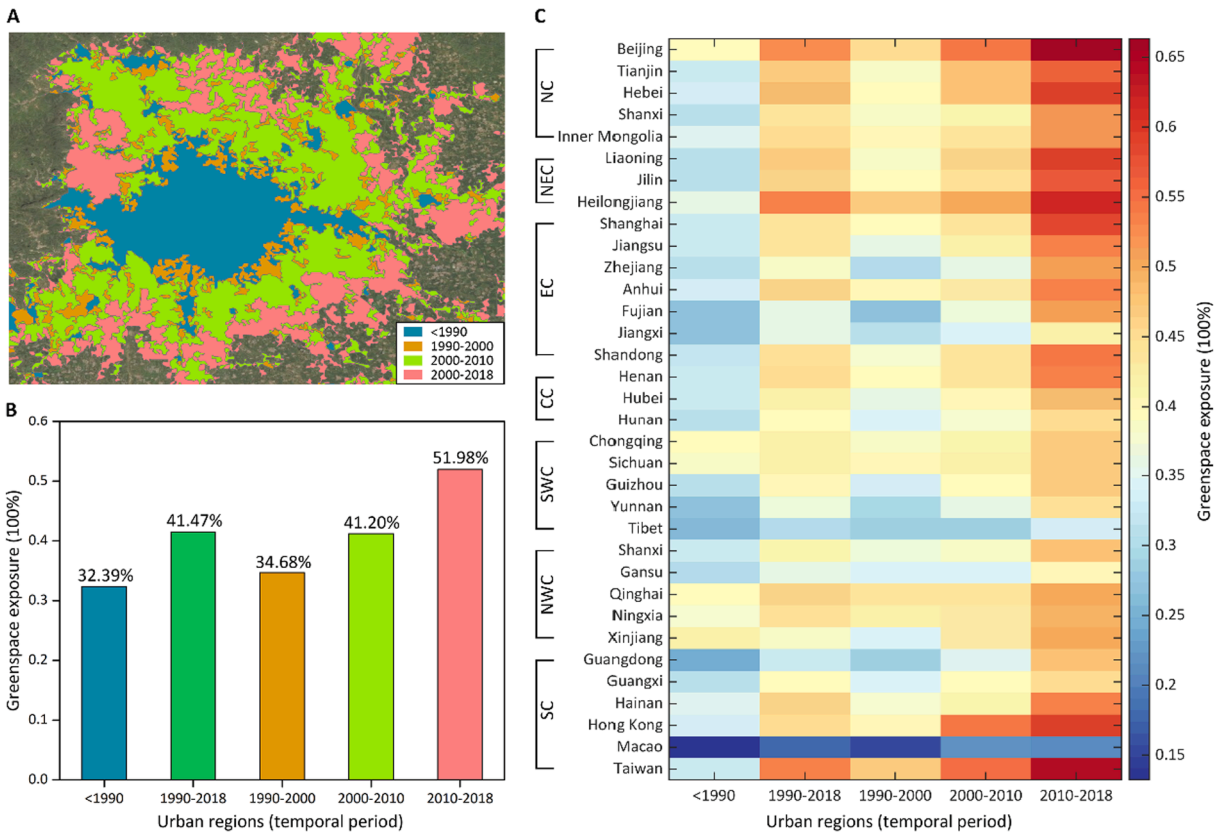

Fig. 8. Urban expansion and greenspace exposure changes. (A) Urban expansion procedure from 1990 to 2018 in Beijing, (B) the levels of greenspace exposure in urban areas with different temporal periods for entire China, and (C) for individual province.

However, this is not exactly equal to the physical accessibility to green spaces regarding the property right (private greenspace such as private backyards, community gardens, and parks) and the inaccessibility in the contexts of high-rise and dense urban settings (Sun et al., 2021). We also acknowledge that it would be more accurate and comprehensive to consider the socioeconomic status and population structure into the greenspace exposure assessment, since several empirical studies at local scales of communities or cities have revealed the impacts of people's lifestyle priority and socioeconomic status on the real utilization of greenspace (Dadvand et al., 2012; Mueller et al., 2018; Olsen et al., 2022). Nevertheless, the distance between people and nearby greenspace has been widely recognized as the detrimental factor on human exposure to greenspace and the associated health benefits (Abareshi et al., 2020; Markevych et al., 2014; Nutsford et al., 2013), which reinforces the presumption of this study to focus on the spatial interaction between people and greenspace. Overall, this study provides a comprehensive understanding of physical greenspace distribution and human greenspace exposure in China, which serves as a benchmark that a wide range of future research, practices, and optimizations can be incorporated with.

5. Conclusions

This nationwide study is part of an effort to examine multi-scale differences of human exposure to greenspace across provinces, cities, counties, towns, and land parcels in China. We find a prominent scaling effect of greenspace exposure difference across multi-scale administrative divisions that greenspace exposure will be more spatially heterogeneous with the lens of finer-scale assessments. Our results reveal that the greenspace coverage rate will be biased to reflect realistic human greenspace exposure levels. An asymmetric pattern of the difference between greenspace exposure and greenspace coverage at the two sides of Heihe–Tengchong Line is identified. Specifically, the greenspace coverage rate will generally overestimate people's real exposure to greenspace in East China and underestimate in West China. We also identify urbanization is associated with the spatial gradient in greenspace exposure difference. By comparing greenspace exposures among urbanized areas from 1990 to 2018, our results reveal that the newly urbanized areas are experiencing much better greenspace exposure than the old urban areas. The deliverables from this study including data, method, and information will be informative and supportive for policymakers, city planners, and landscape architects to facilitate sustainable and healthy urban planning and management.

6. Open data policy

The fractional greenspace coverage maps for China in 2020 and the multi-scale assessment results of greenspace exposure across scales of province, city, county, town, and land parcel in China are available for download and visualization here (https://fuselab.hku.hk).

CRediT authorship contribution statement

Bin Chen: Conceptualization, Data curation, Formal analysis, Methodology, Software, Writing – original draft. **Ying Tu:** Data curation, Methodology. **Shengbiao Wu:** Data curation, Methodology, Validation. **Yimeng Song:** Writing – review & editing. **Yufang Jin:** Writing – review & editing. **Chris Webster:** Writing – review & editing. **Bing Xu:** Writing – review & editing. **Peng Gong:** Writing – review & editing.

Declaration of Competing Interest

The authors declare that they have no known competing financial interests or personal relationships that could have appeared to influence

the work reported in this paper.

Acknowledgements

This study was supported by the University of Hong Kong HKU-100 Scholars Fund and URC Small Equipment Grant (012530228), Major Program of the National Natural Science Foundation of China (42090015, 72091514), the National Natural Science Foundation of China (42071400), and Tsinghua-Toyota Joint Research Fund. The authors would like to thank two anonymous reviewers and editors for providing valuable suggestions and comments, which have greatly improved this manuscript.

Appendix A. Supplementary material

Supplementary data to this article can be found online at https://doi.org/10.1016/j.envint.2022.107348.

References

Addas, A., Maghrabi, A., 2022. How did the COVID-19 pandemic impact urban green spaces? A multi-scale assessment of Jeddah megacity (Saudi Arabia). Urban For. Urban Greening 69, 127493. https://doi.org/10.1016/j.ufug.2022.127493.

Abareshi, F., Sharifi, Z., Hekmatshoar, R., Fallahi, M., Lari Najafi, M., Ahmadi Asour, A., Mortazavi, F., Akrami, R., Miri, M., Dadvand, P., 2020. Association of exposure to air pollution and green space with ovarian reserve hormones levels. Environ. Res. 184, 109342. https://doi.org/10.1016/j.envres.2020.109342.

Cameron, R., Hitchmough, J. (2016). Environmental horticulture: science and management of green landscapes. CAB International, Boston: MA.

Chen, B., Nie, Z., Chen, Z., Xu, B., 2017. Quantitative estimation of 21st-century urban greenspace changes in Chinese populous cities. Sci. Total Environ. 609, 956–965. https://doi.org/10.1016/j.scitotenv.2017.07.238.

Chen, B., Song, Y., Jiang, T., Chen, Z., Huang, B.o., Xu, B., 2018a. Real-time estimation of population exposure to PM2.5 using mobile- and station-based big data. Int. J. Environ. Res. Public Health 15 (4), 573. https://doi.org/10.3390/ijerph15040573.

Chen, B., Song, Y., Kwan, M.-P., Huang, B.o., Xu, B., 2018b. How do people in different places experience different levels of air pollution? Using worldwide Chinese as a lens. Environ. Pollut. 238, 874–883. https://doi.org/10.1016/j.envpol.2018.03.093.

Chen, Y., Yue, W., La Rosa, D., 2020. Which communities have better accessibility to green space? An investigation into environmental inequality using big data. Landscape Urban Plann. 204, 103919. https://doi.org/10.1016/j.landurbplan.2020.103919.

Chi, W., Jia, J., Pan, T., Jin, L., Bai, X., 2020. Multi-scale analysis of green space for human settlement sustainability in urban areas of the inner Mongolia Plateau, China. Sustainability 12 (17), 6783. https://doi.org/10.3390/su12176783.

Collins, R.M., Spake, R., Brown, K.A., Ogutu, B.O., Smith, D., Eigenbrod, F., 2020. A systematic map of research exploring the effect of greenspace on mental health. Landscape Urban Plann. 201, 103823. https://doi.org/10.1016/j.landurbplan.2020.103823.

CIESIN (2018). Gridded Population of the World, Version 4 (GPWv4): Population Count, Revision 11. NASA Socioeconomic Data and Applications Center (SEDAC). Palisades, NY.

Dadvand, P., de Nazelle, A., Figueras, F., Basagaña, X., Su, J., Amoly, E., Jerrett, M., Vrijheid, M., Sunyer, J., Nieuwenhuijsen, M.J., 2012. Green space, health inequality and pregnancy. Environ. Int. 40, 110–115.

Dobson, J.E., Bright, E.A., Coleman, P.R., Durfee, R.C., Worley, B.A., 2000. LandScan: a global population database for estimating populations at risk. Photogramm. Eng. Remote Sens. 66, 849–857.

Doick, K.J., Peace, A., Hutchings, T.R., 2014. The role of one large greenspace in mitigating London's nocturnal urban heat island. Sci. Total Environ. 493, 662–671.

Ezzati, M., Webster, C.J., Doyle, Y.G., Rashid, S., Owusu, G., Leung, G.M., 2018. Cities for global health. BMJ 363, k3794.

Francis, J., Giles-Corti, B., Wood, L., Knuiman, M., 2012. Creating sense of community: The role of public space. J. Environ. Psychol. 32 (4), 401–409.

Friedlingstein, P., O'Sullivan, M., Jones, M.W., Andrew, R.M., Hauck, J., Olsen, A., Peters, G.P., Peters, W., Pongratz, J., Sitch, S., Le Quéré, C., Canadell, J.G., Ciais, P., Jackson, R.B., Alin, S., Aragão, L.E.O.C., Arneth, A., Arora, V., Bates, N.R., Becker, M., Benoit-Cattin, A., Bittig, H.C., Bopp, L., Bultan, S., Chandra, N., Chevallier, F., Chini, L.P., Evans, W., Florentie, L., Forster, P.M., Gasser, T., Gehlen, M., Gilfillan, D., Gkritzalis, T., Gregor, L., Gruber, N., Harris, I., Hartung, K., Haverd, V., Houghton, R.A., Ilyina, T., Jain, A.K., Joetzjer, E., Kadono, K., Kato, E., Kitidis, V., Korsbakken, J.I., Landschützer, P., Lefèvre, N., Lenton, A., Lienert, S., Liu, Z., Lombardozzi, D., Marland, G., Metzl, N., Munro, D.R., Nabel, J.E.M.S., Nakaoka, S.-I., Niwa, Y., O'Brien, K., Ono, T., Palmer, P.I., Pierrot, D., Poulter, B., Resplandy, L., Robertson, E., Rödenbeck, C., Schwinger, J., Séférian, R., Skjelvan, I., Smith, A.J.P., Sutton, A.J., Tanhua, T., Tans, P.P., Tian, H., Tilbrook, B., van der Werf, G., Vuichard, N., Walker, A.P., Wanninkhof, R., Watson, A.J., Willis, D., Wiltshire, A.J., Yuan, W., Yue, X.u., Zaehle, S., 2020. Global carbon budget 2020. Earth Syst. Sci. Data 12 (4), 3269–3340.

Gong, P., Chen, B., Li, X., Liu, H., Wang, J., Bai, Y., Chen, J., Chen, X.i., Fang, L., Feng, S., Feng, Y., Gong, Y., Gu, H., Huang, H., Huang, X., Jiao, H., Kang, Y., Lei, G., Li, A., Li, X., Li, X., Li, Y., Li, Z., Li, Z., Liu, C., Liu, C., Liu, M., Liu, S., Mao, W., Miao, C., Ni, H., Pan, Q., Qi, S., Ren, Z., Shan, Z., Shen, S., Shi, M., Song, Y., Su, M.o., Ping Suen, H., Sun, B.o., Sun, F., Sun, J., Sun, L., Sun, W., Tian, T., Tong, X., Tseng, Y., Tu, Y., Wang, H., Wang, L., Wang, X.i., Wang, Z., Wu, T., Xie, Y., Yang, J., Yang, J., Yuan, M., Yue, W., Zeng, H., Zhang, K., Zhang, N., Zhang, T., Zhang, Y.u., Zhao, F., Zheng, Y., Zhou, Q., Clinton, N., Zhu, Z., Xu, B., 2020a. Mapping essential urban land use categories in China (EULUC-China): Preliminary results for 2018. Sci. Bull. 65 (3), 182–187.

Gong, P., Li, X., Wang, J., Bai, Y., Chen, B., Hu, T., Liu, X., Xu, B., Yang, J., Zhang, W., Zhou, Y., 2020b. Annual maps of global artificial impervious area (GAIA) between 1985 and 2018. Remote Sens. Environ. 236, 111510. https://doi.org/10.1016/j.rse.2019.111510.

Gong, P., Liang, S., Carlton, E.J., Jiang, Q., Wu, J., Wang, L., Remais, J.V., 2012. Urbanisation and health in China. The Lancet 379 (9818), 843–852.

Hu, H., 1935. Distribution of China's population: Accompanying charts and density map. Acta Geographica Sinica 2, 33–74.

Jennings, V., Johnson Gaither, C., Gragg, R.S., 2012. Promoting environmental justice through urban green space access: A synopsis. Environ. Justice 5 (1), 1–7.

Jiang, B., Deal, B., Pan, H., Larsen, L., Hsieh, C.-H., Chang, C.-Y., Sullivan, W.C., 2017. Remotely-sensed imagery vs. eye-level photography: Evaluating associations among measurements of tree cover density. Landscape Urban Plann. 157, 270–281.

Jiang, B., Li, D., Larsen, L., Sullivan, W.C., 2016. A dose-response curve describing the relationship between urban tree cover density and self-reported stress recovery. Environ. Behavior 48 (4), 607–629.

Jim, C.Y., Chen, S.S., 2003. Comprehensive greenspace planning based on landscape ecology principles in compact Nanjing city, China. Landscape Urban Plann. 65 (3), 95–116.

Kabisch, N., Haase, D., 2013. Green spaces of European cities revisited for 1990–2006. Landscape Urban Plann. 110, 113–122.

Kemperman, A., Timmermans, H., 2014. Green spaces in the direct living environment and social contacts of the aging population. Landscape Urban Plann. 129, 44–54.

Keshava, N., 2003. A survey of spectral unmixing algorithms. Lincoln Laborat. J. 14, 55–78.

Kuang, W., Zhang, S., Li, X., Lu, D., 2021. A 30 m resolution dataset of China's urban impervious surface area and green space, 2000–2018. Earth Syst. Sci. Data 13, 63–82.

Kumar, P., Druckman, A., Gallagher, J., Gatersleben, B., Allison, S., Eisenman, T.S., Hoang, U.y., Hama, S., Tiwari, A., Sharma, A., Abhijith, K.V., Adlakha, D., McNabola, A., Astell-Burt, T., Feng, X., Skeldon, A.C., de Lusignan, S., Morawska, L., 2019. The nexus between air pollution, green infrastructure and human health. Environ. Int. 133, 105181. https://doi.org/10.1016/j.envint.2019.105181.

Labib, S.M., Lindley, S., Huck, J.J., 2020. Scale effects in remotely sensed greenspace metrics and how to mitigate them for environmental health exposure assessment. Computers Environ. Urban Syst. 82, 101501. https://doi.org/10.1016/j.compenvurbsys.2020.101501.

Li, X., Gong, P., Zhou, Y., Wang, J., Bai, Y., Chen, B., Hu, T., Xiao, Y., Xu, B., Yang, J., Liu, X., Cai, W., Huang, H., Wu, T., Wang, X.i., Lin, P., Li, X., Chen, J., He, C., Li, X., Yu, L.e., Clinton, N., Zhu, Z., 2020. Mapping global urban boundaries from the global artificial impervious area (GAIA) data. Environ. Res. Lett. 15 (9), 094044. https://doi.org/10.1088/1748-9326/ab9be3.

Liou, Y.-A., Nguyen, K.-A., Ho, L.-T., 2021. Altering urban greenspace patterns and heat stress risk in Hanoi city during Master Plan 2030 implementation. Land Use Policy 105, 105405. https://doi.org/10.1016/j.landusepol.2021.105405.

Liu, H., Remme, R.P., Hamel, P., Nong, H., Ren, H., 2020. Supply and demand assessment of urban recreation service and its implication for greenspace planning-A case study on Guangzhou. Landscape Urban Plann. 203, 103898. https://doi.org/10.1016/j.landurbplan.2020.103898.

Lu, Y.i., Chen, L., Liu, X., Yang, Y., Sullivan, W.C., Xu, W., Webster, C., Jiang, B., 2021. Green spaces mitigate racial disparity of health: A higher ratio of green spaces indicates a lower racial disparity in SARS-CoV-2 infection rates in the USA. Environ. Int. 152, 106465. https://doi.org/10.1016/j.envint.2021.106465.

Maimaitiyiming, M., Ghulam, A., Tiyip, T., Pla, F., Latorre-Carmona, P., Halik, Ü., Sawut, M., Caetano, M., 2014. Effects of green space spatial pattern on land surface temperature: Implications for sustainable urban planning and climate change adaptation. ISPRS J. Photogramm. Remote Sens. 89, 59–66.

Markevych, I., Schoierer, J., Hartig, T., Chudnovsky, A., Hystad, P., Dzhambov, A.M., de Vries, S., Triguero-Mas, M., Brauer, M., Nieuwenhuijsen, M.J., Lupp, G., Richardson, E.A., Astell-Burt, T., Dimitrova, D., Feng, X., Sadeh, M., Standl, M., Heinrich, J., Fuertes, E., 2017. Exploring pathways linking greenspace to health: Theoretical and methodological guidance. Environ. Res. 158, 301–317.

Markevych, I., Tiesler, C.M.T., Fuertes, E., Romanos, M., Dadvand, P., Nieuwenhuijsen, M.J., Berdel, D., Koletzko, S., Heinrich, J., 2014. Access to urban green spaces and behavioural problems in children: Results from the GINIplus and LISAplus studies. Environ. Int. 71, 29–35.

Melero, Y., Stefanescu, C., Palmer, S.C.F., Travis, J.M.J., Pino, J., 2020. The role of the urban landscape on species with contrasting dispersal ability: Insights from greening plans for Barcelona. Landscape Urban Plann. 195, 103707. https://doi.org/10.1016/j.landurbplan.2019.103707.

Mitchell, R., Popham, F., 2008. Effect of exposure to natural environment on health inequalities: an observational population study. The Lancet 372 (9650), 1655–1660.

Mu, B.o., Liu, C., Tian, G., Xu, Y., Zhang, Y., Mayer, A.L., Lv, R., He, R., Kim, G., 2020. Conceptual planning of urban–rural green space from a multidimensional perspective: A case study of Zhengzhou, China. Sustainability 12 (7), 2863. https://doi.org/10.3390/su12072863.

Mueller, N., Rojas-Rueda, D., Khreis, H., Cirach, M., Milà, C., Espinosa, A., Foraster, M., McEachan, R.R.C., Kelly, B., Wright, J., Nieuwenhuijsen, M., 2018. Socioeconomic inequalities in urban and transport planning related exposures and mortality: a health impact assessment study for Bradford, UK. Environ. Int. 121, 931–941.
Nowak, D.J., Greenfield, E.J., 2012. Tree and impervious cover change in US cities. Urban For. Urban Greening 11 (1), 21–30.
Nowak, D.J., Hirabayashi, S., Bodine, A., Greenfield, E., 2014. Tree and forest effects on air quality and human health in the United States. Environ. Pollut. 193, 119–129.
Nutsford, D., Pearson, A.L., Kingham, S., 2013. An ecological study investigating the association between access to urban green space and mental health. Public Health 127 (11), 1005–1011.
Olsen, J.R., Caryl, F.M., McCrorie, P., Mitchell, R., 2022. Socioeconomic inequality in Scottish children's exposure to and use of natural space and private gardens, measured by GPS. Landscape Urban Plann. 223, 104425.
Reid, C., Clougherty, J., Shmool, J., Kubzansky, L., 2017. Is all urban green space the same? A comparison of the health benefits of trees and grass in New York City. Int. J. Environ. Res. Public Health 14 (11), 1411. https://doi.org/10.3390/ijerph14111411.
Rigolon, A., Browning, M., Jennings, V., 2018. Inequities in the quality of urban park systems: An environmental justice investigation of cities in the United States. Landscape Urban Plann. 178, 156–169.
Rutt, R.L., Gulsrud, N.M., 2016. Green justice in the city: A new agenda for urban green space research in Europe. Urban For. Urban Greening 19, 123–127.
Sarkar, C., Webster, C., Gallacher, J., 2018. Residential greenness and prevalence of major depressive disorders: a cross-sectional, observational, associational study of 94 879 adult UK Biobank participants. The Lancet Planetary Health 2, e162–e173.
Sathyakumar, V., Ramsankaran, RAAJ, Bardhan, R., 2019. Linking remotely sensed Urban Green Space (UGS) distribution patterns and Socio-Economic Status (SES)-A multi-scale probabilistic analysis based in Mumbai, India. GIScience Remote Sens. 56 (5), 645–669.
Song, Y., Chen, B., Ho, H.C., Kwan, M.-P., Liu, D., Wang, F., Wang, J., Cai, J., Li, X., Xu, Y., He, Q., Wang, H., Xu, Q., Song, Y., 2021. Observed inequality in urban greenspace exposure in China. Environ. Int. 156, 106778. https://doi.org/10.1016/j.envint.2021.106778.
Song, Y., Chen, B., Kwan, M.-P., 2020. How does urban expansion impact people's exposure to green environments? A comparative study of 290 Chinese cities. J. Cleaner Prod. 246, 119018. https://doi.org/10.1016/j.jclepro.2019.119018.
Song, Y., Huang, B.o., Cai, J., Chen, B., 2018. Dynamic assessments of population exposure to urban greenspace using multi-source big data. Sci. Total Environ. 634, 1315–1325. https://doi.org/10.1016/j.scitotenv.2018.04.061.
Stevens, F.R., Gaughan, A.E., Linard, C., & Tatem, A.J. (2015). Disaggregating census data for population mapping using random forests with remotely-sensed and ancillary data. PLoS One, *10*, e0107042.
Strohbach, M.W., Lerman, S.B., Warren, P.S., 2013. Are small greening areas enhancing bird diversity? Insights from community-driven greening projects in Boston. Landscape Urban Plann. 114, 69–79.
Su, J.G., Dadvand, P., Nieuwenhuijsen, M.J., Bartoll, X., Jerrett, M., 2019. Associations of green space metrics with health and behavior outcomes at different buffer sizes and remote sensing sensor resolutions. Environ. Int. 126, 162–170.
Sun, G., Webster, C., Zhang, X., 2021. Connecting the city: a three-dimensional pedestrian network of Hong Kong. Environ. Plann. B: Urban Anal. City Sci. 48 (1), 60–75.
Sun, J., Wang, X., Chen, A., Ma, Y., Cui, M., Piao, S., 2011. NDVI indicated characteristics of vegetation cover change in China's metropolises over the last three decades. Environ. Monit. Assess. 179 (1-4), 1–14.
Sun, Y., Xie, S., Zhao, S., 2019. Valuing urban green spaces in mitigating climate change: A city-wide estimate of aboveground carbon stored in urban green spaces of China's Capital. Glob. Change Biol. 25 (5), 1717–1732.
Theobald, D.M., Kennedy, C., Chen, B., Oakleaf, J., Baruch-Mordo, S., Kiesecker, J., 2020. Earth transformed: detailed mapping of global human modification from 1990 to 2017. Earth Syst. Sci. Data 12 (3), 1953–1972.
Tu, Y., Chen, B., Yu, L.e., Xin, Q., Gong, P., Xu, B., 2021. How does urban expansion interact with cropland loss? A comparison of 14 Chinese cities from 1980 to 2015. Landscape Ecol. 36 (1), 243–263.
Wang, J., Zhou, W., Wang, J., Yu, W., 2020. Spatial distribution of urban greenspace in response to urban development from a multi-scale perspective. Environ. Res. Lett. 15 (6), 064031. https://doi.org/10.1088/1748-9326/ab719f.
Weng, Q., Lu, D., Schubring, J., 2004. Estimation of land surface temperature–vegetation abundance relationship for urban heat island studies. Remote Sens. Environ. 89 (4), 467–483.
Wolch, J.R., Byrne, J., Newell, J.P., 2014. Urban green space, public health, and environmental justice: The challenge of making cities 'just green enough'. Landscape Urban Plann. 125, 234–244.
Wu, L., Kim, S.K., 2021. Exploring the equality of accessing urban green spaces: A comparative study of 341 Chinese cities. Ecol. Ind. 121, 107080. https://doi.org/10.1016/j.ecolind.2020.107080.
Wüstemann, H., Kalisch, D., Kolbe, J., 2017. Access to urban green space and environmental inequalities in Germany. Landscape Urban Plann. 164, 124–131.
Xu, C., Haase, D., Pribadi, D.O., Pauleit, S., 2018. Spatial variation of green space equity and its relation with urban dynamics: A case study in the region of Munich. Ecol. Ind. 93, 512–523.
Yang, J., Huang, C., Zhang, Z., Wang, L.e., 2014. The temporal trend of urban green coverage in major Chinese cities between 1990 and 2010. Urban For. Urban Greening 13 (1), 19–27.
Young, R.F., 2010. Managing municipal green space for ecosystem services. Urban For. Urban Greening 9 (4), 313–321.
Zhao, J., Chen, S., Jiang, B.o., Ren, Y., Wang, H., Vause, J., Yu, H., 2013. Temporal trend of green space coverage in China and its relationship with urbanization over the last two decades. Sci. Total Environ. 442, 455–465.
Zhao, K., Jackson, R.B., 2014. Biophysical forcings of land-use changes from potential forestry activities in North America. Ecol. Monogr. 84 (2), 329–353.
Zhou, Q., Konijnendijk van den Bosch, C.C., Chen, Z., Wang, X., Zhu, L., Chen, J., Lin, Y., Dong, J., 2021. China's Green space system planning: Development, experiences, and characteristics. Urban For. Urban Greening 60, 127017. https://doi.org/10.1016/j.ufug.2021.127017.